Journal of Macromolecular Science, Part A
Publication details, including instructions for authors and subscription information:
http://www.informaworld.com/smpp/title~content=t713597274

Characterizations of Thermoplastic Block Elastomers Based on Polybutadiene and ε -Caprolactone

Michael Lemoine[a]; Claire-Helene Brachais[a]; Gilles Boni[a]; Laurent Brachais[b]; Jean-Pierre Couvercelle[a]
[a] Institut de Chimie Moléculaire de l'Université de Bourgogne, Systèmes HYbrides Multifonctionnels, Université de Bourgogne, Dijon, France [b] EMMA, ENSBANA, Université de Bourgogne, Dijon, France

Online publication date: 05 July 2010

To cite this Article Lemoine, Michael , Brachais, Claire-Helene , Boni, Gilles , Brachais, Laurent and Couvercelle, Jean-Pierre(2010) 'Characterizations of Thermoplastic Block Elastomers Based on Polybutadiene and ε -Caprolactone', Journal of Macromolecular Science, Part A, 47: 8, 794 — 803
To link to this Article: DOI: 10.1080/10601325.2010.492041
URL: http://dx.doi.org/10.1080/10601325.2010.492041

Journal of Macromolecular Science, Part A: Pure and Applied Chemistry (2010) **47**, 794–803

ISSN: 1060-1325 print / 1520-5738 online
DOI: 10.1080/10601325.2010.492041

Taylor & Francis
Taylor & Francis Group

Characterizations of Thermoplastic Block Elastomers Based on Polybutadiene and ε-Caprolactone

MICHAEL LEMOINE[1,*], CLAIRE-HELENE BRACHAIS[1], GILLES BONI[1], LAURENT BRACHAIS[2], and JEAN-PIERRE COUVERCELLE[1]

[1]*Institut de Chimie Moléculaire de l'Université de Bourgogne, Systèmes HYbrides Multifonctionnels, Université de Bourgogne, Dijon, France*
[2]*EMMA, ENSBANA, Université de Bourgogne, esplanade AGROSuP, Dijon, France*

Received February 2010, Accepted March 2010

A broad series of tri- and multiblock copolymers based on linear and branched oligomers of polybutadiene as central blocks and polycaprolactone (PCL) as block extremities are characterized by SEC, DSC, DMA, Dynamical Rheology and DRX. DSC analyses reveal phase separation between the two amorphous PB and PCL phases. By thermal analysis, the glass transition temperature of PCL is only detected for materials containing at least 80% w/w of PCL. This is attributed to the small length of the polyester blocks for copolymers containing less than 80% w/w of PCL. The increase of fusion heat with increasing PCL content in the copolymers is correlated to the greater ability of PCL chains to rearrange as HTPB amount decrease in the material. Regarding the evolution of the melting temperature of the various copolymers, the characterization by DMA and dynamical rheology confirms the behaviour observed by DSC. Mechanical and rheological properties (i.e., storage modulus and complex viscosities) were studied and reveal that the behavior of the copolymers depends on both the rate of PCL chains and on the nature of the elastomeric block.

Keywords: PB-PCL copolymers, thermal properties, mechanical properties, complex viscosity

1 Introduction

Thermoplastic elastomers (TPEs) are characterized by a heterogenic structure with both soft and hard immiscible segments. Soft segments are responsible for the elastic behavior of the corresponding polymeric block whereas hard segments allow the mechanical cohesion of the material (1). Due to this specific architecture, these materials present intermediate properties between those of an elastomer and those of a rigid thermoplastic. Each phase has its own glass transition temperature T_g, which determines the thermal limit of use. Indeed, the T_g of the rigid phase must be higher than the temperature of use while the T_g of the soft phase should be less than the operating temperature. Consequently, these materials show the characteristics of a vulcanized rubber at the operating temperature (i.e., elasticity), and they behave like thermoplastics at the processing temperature (i.e., a softening is observed when heating above their T_g) (2).

Triblock copolymers with an elastomeric central block and glassy end blocks exhibit the properties of thermoplastic elastomers (TPE). The famoust examples are the commercial SBS (3,4,5,6,7,8) or SIS (9,10,11) triblock copolymers and SEBS (12,13,14) copolymers.

These multiblock materials are used in many fields such as biomedical applications (15), sealants (16), electric wires (17) or in adhesive formulations (18). In this last application, the most currently used copolymers are diblock or triblock copolymers of polystyrene and polydiene. The replacement of rigid polystyrene blocks by semi-crystalline blocks (with T_m above room temperature) could be an interesting route to obtain new materials with original properties. As an example, varying the nature of the rigid phase could allow a lower processing temperature of the material. Recently, synthesis of block copolymers based on styrene, butadiene and ε-caprolactone (PS-PB-PCL, PS-PCL and PB-PCL type) has been reported (19). Di or triblock copolymers (PB-PCL or PB-PCL-PB) have been synthetized (20).

In a previous paper (21), we described the synthesis of multi-blocks copolymers based on poly(caprolactone) (PCL) and poly(butadiene) (PB) starting from various hydroxytelechelic poly(butadiene). In this work, PB-PCL

*Address correspondence to: Claire-Helene Brachais, Institut de Chimie Moléculaire de l'Université de Bourgogne, Systèmes HYbrides Multifonctionnels, UMR CNRS 5260, Université de Bourgogne, UFR Sciences et Techniques, 9 Avenue Alain Savary, BP 47870, 21078 Dijon, France. Tel: +33 (0)380393777; Fax: +33 (0)380396098; E-mail: claire-helene.brachais@u-bourgogne.fr

copolymers were synthesized by ring opening polymerisation of ε-caprolactone initiated by macroiniatiator polybutadiene terminated by lithium alkoxide. Depending on the functionality of the HTPB oligomers, the structure of the resulting copolymers is either star-shaped or linear triblocks.

Little research focuses on the synthesis and thermal or mechanical characterization of PB-PCL triblocks. For example, Meng et al (22) worked on the synthesis of PCL-PB-PCL triblocks based on HTPB oligomers and further use of these materials for curing applications. Working on the cristallization of PB-PCL diblock copolymers with various amounts of PB and PCL, Nojima et al (23,24) studied the formation, the organization and the regularity of spherolites by DRX, DSC and optical microscopy**.** Phase separation in multiblocks copolymers, such as PS-PCL, PI-PCL, PS-PB-PC and PS-PI-PCL, was evidenced (9,25,26) using DRX and DMA techniques. Jackson et al (27) studied the surface topology and the organization of PCL crystals in PB-PCL and PS-PB-PCL copolymers. In all these studies, the thermal and mechanical characterizations of PB-PCL multiblocks in relation to their compositions have never been described.

The aim of this work is to characterize mutliblocks copolymers PB-PCL synthesized from various HTPB and containing various amounts of PB and PCL. Four different grades of HTPB are used in this work and all the obtained copolymers are characterized by DSC, DMTA, Dynamical Rheology and DRX.

2 Experimental

2.1 Preparation of the Samples

All the samples were prepared starting from HTPB oligomers and ε-caprolactone following the procedure described elsewhere (21). Four grades of hydroxy telechelic polybutadiene (HTPB) with various functionalities were used. R20LM® HTPB ($\overline{M_n}$ = 1600g/mol, $\overline{fOH}$ = 2, 5), R-2, and R45HT® HTPB ($\overline{M_n}$ = 2800 g/mol, $\overline{fOH}$ = 2, 45), R-4, were kindly supplied by ARKEMA. Nisso-Soda provided G2000 HTPB ($\overline{M_n}$ = 2000 g/mol, $\overline{fOH}$ = 2), G-2, and G3000 HTPB ($\overline{M_n}$ = 3000 g/mol, $\overline{fOH}$ = 2), G-3. After the synthesis, the copolymers were poured in ethanol, filtrated and dried at room temperature during two days.

2.2 Apparatus

SEC analysis were carried out on a Gynkotek P580A apparatus equipped with PolyPore columns from Polymer Laboratories (300*7.5 mm) and an IOTA 2 refractive index detector. Polystyrene standards were used for column calibration. Polymer samples were dissolved in THF (10 mg/mL) and elution was performed at 20°C at a flow rate of 1 mL/min, using THF as solvent.

Nuclear Magnetic Resonance (NMR) spectra were recorded in $CDCl_3$ solutions on a Bruker Avance 300 spectrometer. ^1H measurements were carried out at 300.13 MHz using a classical pulse sequence.

Differential Scanning Calorimetry (DSC) measurements were performed using a Q1000 (TA Instruments). A nitrogen flow of 50 mL/min was maintained through the sample holder assemblies during all runs. The samples (10 mg) were sealed in aluminium pans and first heated from −90°C to 80°C at a rate of 10°C/min in order to anneal physical ageing. After fast cooling to −80°C, a second thermal ramp, similar to the first one, is applied to the sample in order to determine the glass transition temperature (T_g). The PCL T_g is measured at inferior onset and the HTPB T_g is measured at half-C_p. The melting temperature (T_m) was determined from the maximum peak value of the endotherm on the first heating scan. The crystalline rate of the materials (X_{cr}) is obtained from the following formula: $\chi_{cr\,PCL} = \frac{\Delta H_f}{\omega_{PCL} * \Delta H_{100}}$ with ΔH_f as the experimental heat of fusion and ω_{PCL} as the PCL weight fraction in the copolymer. is the heat of fusion of a 100% crystalline PCL. The value obtained from the literature is $\Delta H_{100} = 136{,}1$ J/g for PCL (28).

Dynamical Mechanical Analysis (DMA) measurements were performed using a TA Instruments DMA Q800 in a compression mode over a temperature range from −100°C to 80°C. The heating rate and frequency were fixed at 2°C/min and 1 Hz, respectively. Samples for DMA experiments were prepared using a stainless-steel mold and the sample dimensions were 3*0.8*0.2 cm^3.

Parallel Plate Rheometry (AR 500 of TA Instruments) was used to measure the viscosity of materials as a function of the temperature. The samples are preformed in a hot-press with a thickness of 3 mm (±0.3 mm) and a diameter of 30 mm. The samples are placed in the air gap, then melted and the superior plate is stepped down in order to stick the sample between the two plates (diameter = 25 mm). The samples are then slowly cooled down (about 3°C/min) to room temperature in order to avoid recrystallization of the copolymers in a further heating step. An isotherm step at 30°C is applied to the samples during 3 min and analyses are then performed over a temperature range from 30°C to 80°C. The heating rate, frequency and strain were fixed at 4°C/min, 1 Hz and 1%, respectively.

The X-ray diffraction measurements on powdered samples were performed using an Inel CPS120 diffractometer equipped with a Cu anode and a Ge111 monochromator (Kalpha1 = 1.54 Å). The incidence angle was maintained constant at 8 degrees during the 12 h of acquisition.

3 Results and Discussion

The main characteristics of oligomers used as initial macroiniators and corresponding central block are reported in Table 1. It is clear that the oligomers of HTPB

Table 1. Thermal characteristics and microstructures of the starting HTPB oligomers

	HTPB -R2	*HTPB -R4*	*HTPB -G2*	*HTPB -G3*
$\overline{M_n}$(g/mol) (Tonometry)	1 600	2 800	2 000	3 000
$\overline{M_n}$(g/mol) (SEC)	2 200	4 500	4 600	6 300
PDI (SEC)	2.5	2.8	1.3	1.3
1–2 % (^{1}H-NMR)	21	22	85	90
1–4 % (^{1}H-NMR)	79	78	15	10
$\bar{f}_{OH}$	2.6	2.45	2,0	2,0
T_g (°C) (DSC)	−79	−78	−25	−16

Table 2. Compositions and molecular weights for synthesized PB-PCL copolymers

HTPB grade	*PB(%w/w) ^{1}H-NMR*	*PCL(%w/w) ^{1}H-NMR*	*SEC analysis: $\overline{M_n}$ et $\overline{M_w}$(g/mol)*
-R4	60	40	$\overline{M_n} = 11500 \overline{M_w} = 19000$ PDI = 1,6
	35	65	$\overline{M_n} = 14000 \overline{M_w} = 22000$ PDI = 1,6
	20	80	$\overline{M_n} = 20000 \overline{M_w} = 35000$ PDI = 1,8
-R2	35	65	$\overline{M_n} = 9000 \overline{M_w} = 12000$ PDI =1,3
	20	80	$\overline{M_n} = 10000 \overline{M_w} = 14000$ PDI =1,4
-G2	60	40	$\overline{M_n} = 10000 \overline{M_w} = 12000$ PDI = 1,2
	35	65	$\overline{M_n} = 12000 \overline{M_w} = 14500$ PDI = 1,2
	20	80	$\overline{M_n} = 14000 \overline{M_w} = 19000$ PDI = 1,4
-G3	60	40	$\overline{M_n} = 10000 \overline{M_w} = 12500$ PDI = 1,2
	35	65	$\overline{M_n} = 12000 \overline{M_w} = 16000$ PDI =1,3
	20	80	$\overline{M_n} = 18000 \overline{M_w} = 24000$ PDI =1,4

can be classified into two categories according to their functionality. The HTPB R series has functionality strictly greater than 2, while the functionality for the G series is equal to 2. The HTPB R series will lead to star-shaped copolymers while the HTPB G series will be the source of pure tri-blocks copolymers. Because of the variation of the microstructures (1–2 or 1–4 repetition unit contents), the glass transition temperatures of the oligomers vary from −80°C for HTPB -R4 to −16°C for HTPB -G3. The differences of polydispersity refer to the polymerization route. Indeed, HTPB -R4 is derived from a radical polymerization mechanism leading to high PDI values while HTPB -G3 oligomers result from the anionic polymerization of butadiene.

Following the synthesis route described in a previous work (21), block elastomers based on polybutadiene and polycaprolactone are obtained. These materials contain various polycaprolactone rates: 40% w/w, 65% w/w or 80% w/w calculated by ^{1}H-NMR. As the length of HTPB block is fixed, the rate of PCL in the copolymer only depends on the length of the PCL block. Table 2 shows the results obtained from SEC and ^{1}H-NMR characterizations. For the various samples, $\overline{M_n}$ and $\overline{M_w}$ values are included in a

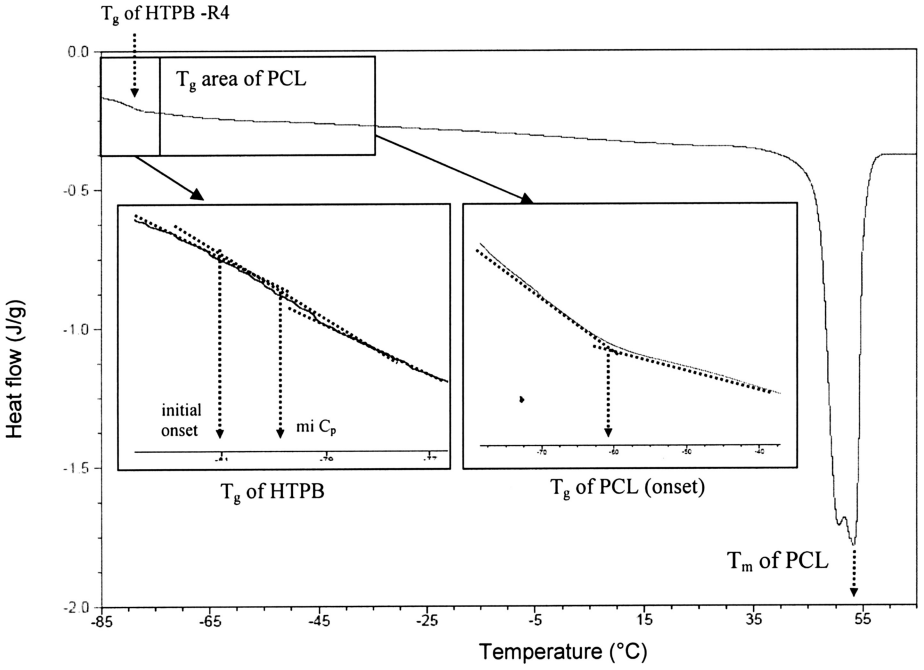

Fig. 1. DSC thermogram of a multi-block copolymer PB-PCL with 20% w/w of HTPB -R4 and 80% w/w of PCL.

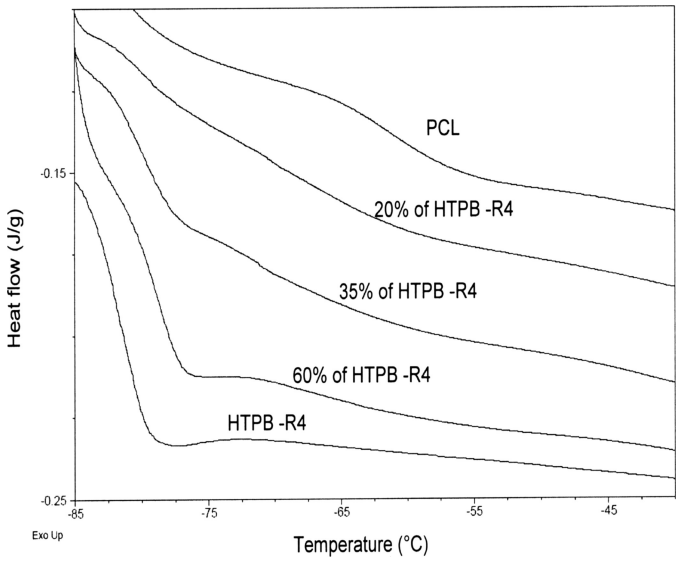

Fig. 2. Temperature range of glass transition for PB-PCL copolymers with different compositions of PB based on HTPB -R4.

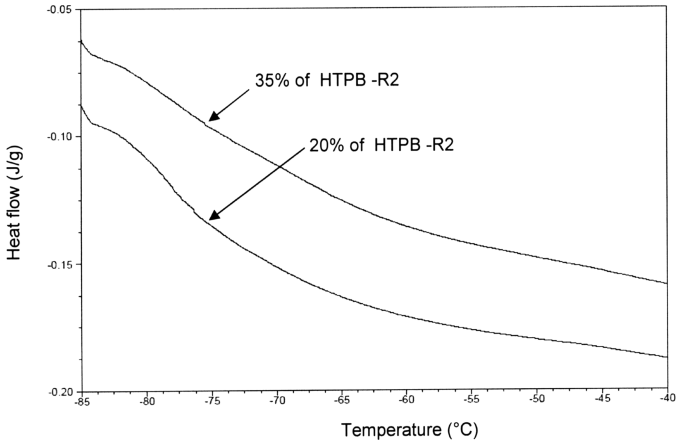

Fig. 4. Temperature range of glass transition for PB-PCL copolymers with different compositions of PB based on HTPB -R2.

range between 9000/20000 g/mol and 12000/35000 g/mol, respectively.

Measurements of glass transition temperatures, variations of fusion heat (ΔH_f) and melt temperatures (T_m) with PCL contents were determined from the DSC heating thermograms (Figs. 1 to 9 and Tables 3 to 6). Two main transitions can be detected corresponding to the glass transition area of the HTPB blocks and the melting peaks of the crystalline PCL phases.

It is well known that pure semi-crystalline PCL displays a glass transition temperature at −60°C (at inferior onset) and a melting peak at 55°C. Glass transition temperatures (determined at half-C_p) for HTPB amorphous homopolymers are easily viewed at −78°C for HTPB -R4 (Fig. 2), −79°C for HTPB -R2 (Table 1), −25°C for HTPB -G2 (Table 1) and −16°C for HTPB -G3 (Fig. 8). The glass transition of copolymers of HTPB blocks is observed at the same temperature than the T_g of the amorphous homopolymers (−78°C, −79°C, −25°C, −16°C, respectively). This is an argument in favor of a phase separation between the two amorphous PB and PCL phases. However T_g of PCL is only detected for materials containing at least 80% w/w of PCL although polybutadiene and PCL being immiscible polymers, glass transition temperatures of the two blocks should be easily determined. Indeed, the glass transition temperature area of PCL blocks can be particularly hard to detect for high crystallinity rate materials.

Figure 1 displays the DSC thermograms of PB-PCL copolymers with 20%w/w of HTPB -R4 and 80%w/w of PCL. With a high content of PCL on the copolymers, the glass transition of PCL is clearly viewed at −60°C. The T_g of HTPB is viewed at −81°C at the initial onset. For the copolymers based on HTPB -R4 and -G3, the T_g of PCL is respectively −61°C and −58°C. In addition, the length of PCL blocks influences the position of T_g. Indeed, T_g of PCL is not clearly visible below 80%w/w of PCL in

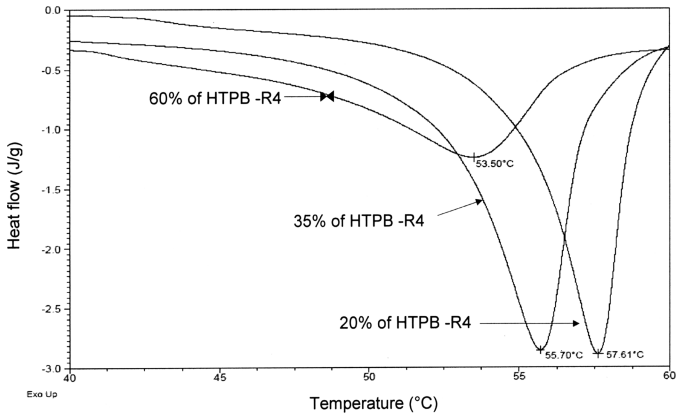

Fig. 3. Temperature range of melting area for PB-PCL copolymers with different compositions of PB based on HTPB -R4.

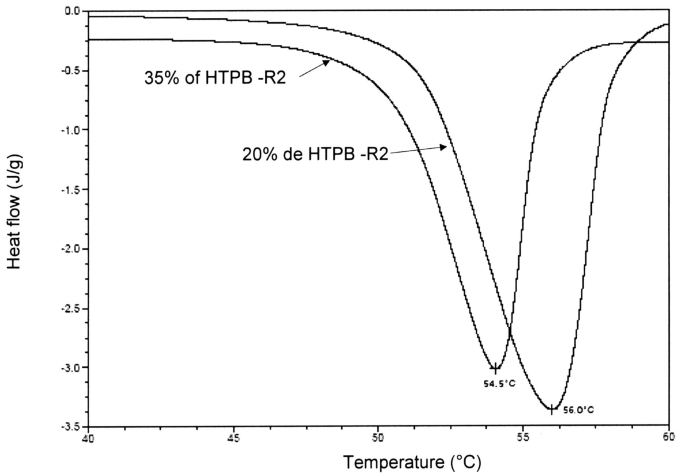

Fig. 5. Temperature range of melting area for PB-PCL copolymers with different compositions of PB based on HTPB -R2.

Table 3. Fusion heat and melting temperature for three copolymers with various amounts of PCL and HTPB -R4

%PB -R4 (w/w)	*%PCL (w/w) (overall)*	T_m(°C)	ΔH_f (J/g)	$\%PCL_{crystalline}$ (w/w)	$\%PCL_{amorphous}$ (w/w)
20	80	58	65	38	42
35	65	56	54	26	39
60	40	53	39	11	29

Table 4. Fusion heat and melting temperature for three copolymers with various amounts of PCL and HTPB -R2

%PB -R2 (w/w)	*%PCL (w/w) (overall)*	T_m(°C)	ΔH_f (J/g)	$\%PCL_{crystalline}$ (w/w)	$\%PCL_{amorphous}$ (w/w)
20	80	56	87	51	29
35	65	54	60	29	36

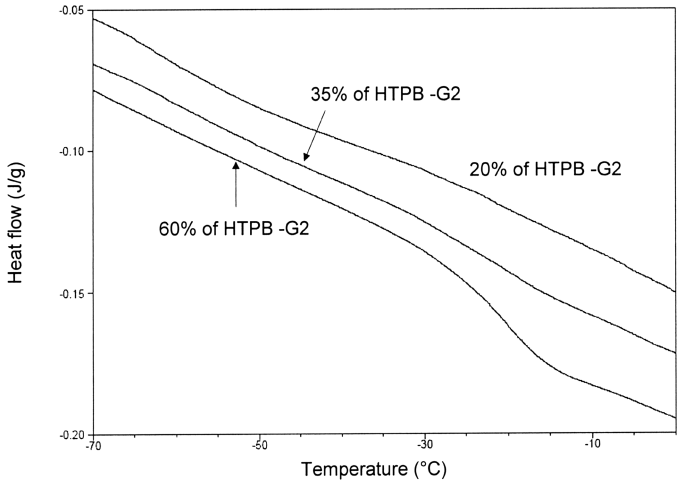

Fig. 6. Temperature range of glass transition for PB-PCL copolymers with different compositions of PB based on HTPB -G2.

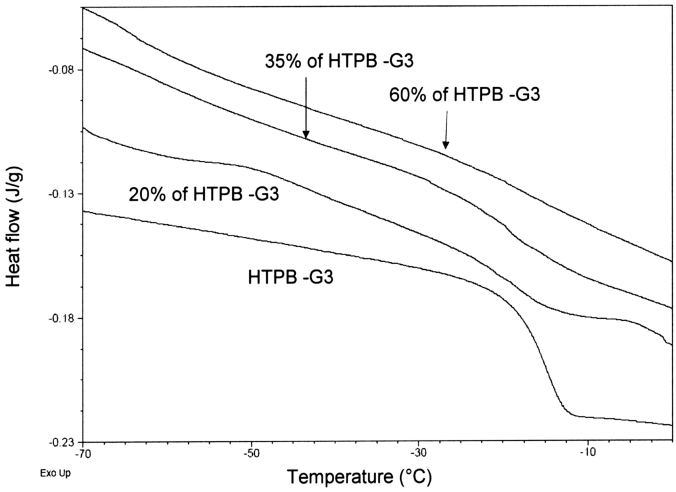

Fig. 8. Temperature range of glass transition and melting area for PB-PCL copolymers with different compositions of PCL and PB based on HTPB -G3.

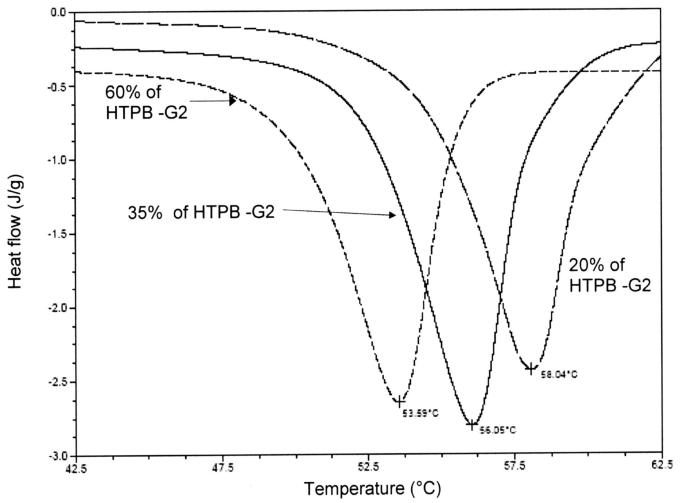

Fig. 7. Temperature range of melting area for PB-PCL copolymers with different compositions of PB based on HTPB -G2.

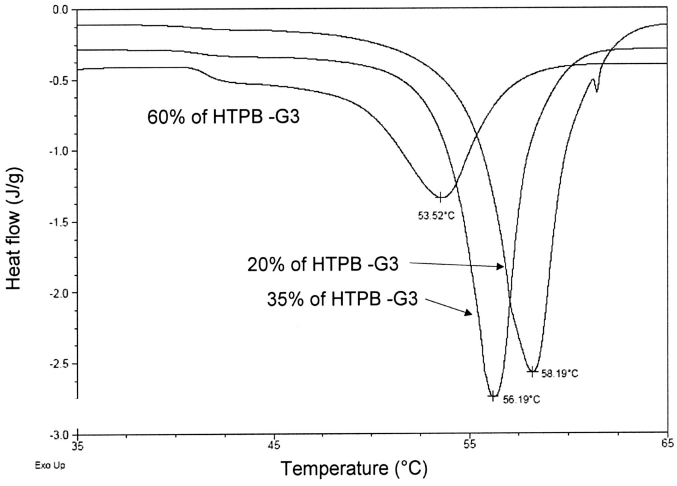

Fig. 9. Temperature range of glass transition and melting area for PB-PCL copolymers with different compositions of PCL and PB based on HTPB -G3.

Table 5. Fusion heat and melting temperature for three copolymers with various amounts of PCL and HTPB -G2

%PB -G2 (w/w)	*%PCL (w/w) (overall)*	T_m(°C)	ΔH_f (J/g)	$\%PCL_{crystalline}$ (w/w)	$\%PCL_{amorphous}$ (w/w)
20	80	58	69	41	39
35	65	56	61	29	36
60	40	54	53	16	24

Table 6. Fusion heat and melting temperature for three copolymers with various amounts of PCL and HTPB -G3

%PB -G3 (w/w)	*%PCL (w/w) (overall)*	T_m(°C)	ΔH_f (J/g)	$\%PCL_{crystalline}$ (w/w)	$\%PCL_{amorphous}$ (w/w)
20	80	58	68	40	40
35	65	56	54	26	39
60	40	53	35	10	30

copolymers. This fact is due to the low content of PCL but also to the small length of the polyester blocks. In the copolymers, the higher the content of PB is, the more important the variation of heat flow for HTPB is.

Tables 3, 4, 5 and 6 display melting temperature (T_m), fusion heat (ΔH_f), crystalline and amorphous PCL ratios in the copolymers for different materials synthesized from the 4 HTPB grades. Concerning the melting areas (Figs. 3, 5 and 7), melting temperatures and fusion heats (Tables 3, 4, 5 and 6) shift to higher values with the increase of PCL content in the materials. As mentioned before, the increase of PCL content is directly related to the higher molecular weight shift of PCL blocks grafted on HTPB. These results are consistent with previous works obtained by Takizawa et al. (29) which have shown that the melting temperature of PCL shifts higher when the molecular weight increases. Typical temperature variations were −20°C for tetramer, 32°C for octamer, 38°C for hexadecamer, 51°C for 32-mer and 54°C for 64-mer. The increase of fusion heat with PCL content in the copolymers is correlated to the amount of PCL crystals in the material and is due to the greater ability of PCL chains to rearrange when HTPB percentage decreases. Thus, it is possible to modulate the thermal properties of the materials by varying the rate of PCL in copolymers.

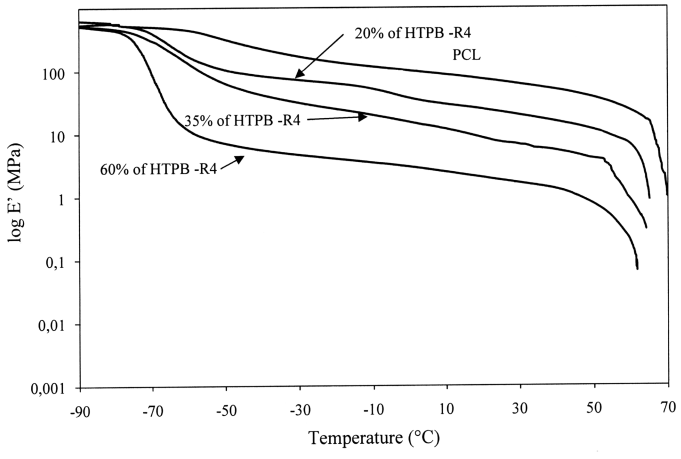

Fig. 10. log E' = f(T) for PB-PCL copolymers with different compositions in weight for PB and PCL synthesized with HTPB -R4 (PCL curve is added for information).

3.1 DMA Measurements

Dynamic mechanical analysis of the copolymers was performed in order to observe the behavior of materials over a large range of temperatures. Figures 10, 12, 14 show the evolution of the storage modulus (log (E')) with the temperature, whereas Figures 11, 13 and 15 show the variation of Tan δ with the temperature for the HTPB -R4, HTPB –G2, HTPB –G3 series. For copolymers synthesized from HTPB -R4 oligomers, below −70°C, the PCL and PB amorphous phases are under their glass transition. Therefore, the materials show a glassy and elastic behavior with a storage modulus superior to 100 MPa. Between −70°C and 40°C, the storage modulus decreases by two decades owing to the glass transitions of the two amorphous phases. The T_g of PCL phase can be detected for the homopolymer at −40°C (Fig. 10) and the T_g of the HTPB -R4 homopolymer can be detected at −70°C in good agreement with Poussard

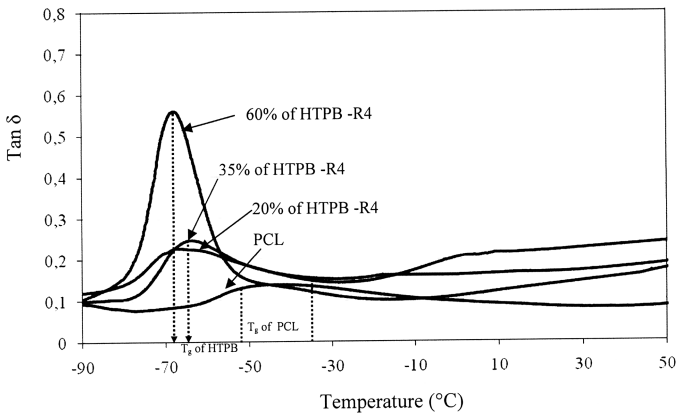

Fig. 11. Tan δ = f(T) for PB-PCL copolymers with different compositions in weight for PB and PCL synthesized with HTPB -R4.

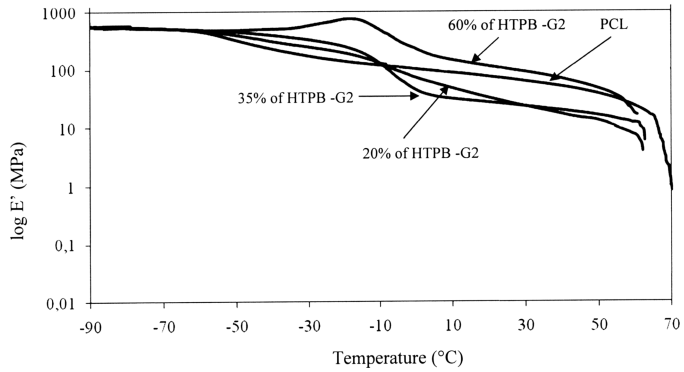

Fig. 12. log E' = f(T) for PB-PCL copolymers with different compositions in weight for PB and PCL synthesized with HTPB -G2.

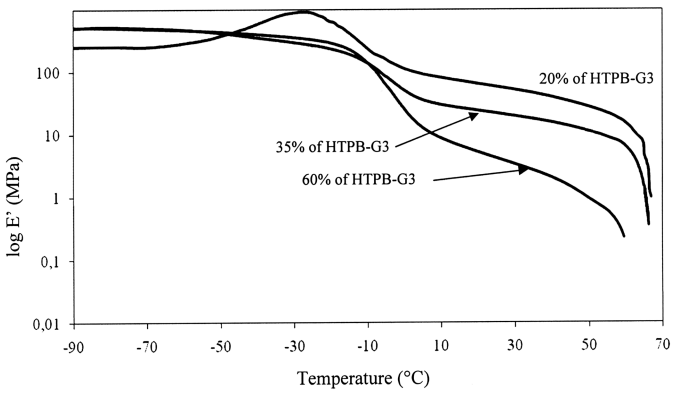

Fig. 14. log E' = f(T) for PB-PCL copolymers with different compositions in weight for PB and PCL synthesized with HTPB -G3.

et al. results (30). As expected, lower storage modulus values are found in the copolymers with higher contents of HTPB. For temperature above 40°C, the melting area corresponds to a drastic decrease of the storage modulus. The evolution of the melting areas (beginning of the fusion) can be related to the PCL amount in the copolymers. As evidenced by previous DSC results, the higher the PCL content, the higher the melting temperature. Similar behavior is observed for copolymers synthesized from HTPB G2000® (Fig. 12) and HTPB G3000® (Fig. 14). In this latter case, the T_g of HTPB blocks is higher (0°C), and the materials show a rigid behavior below −40°C instead of −70°C.

The decrease of the modulus is accompanied by a peak in the viscous dissipation signal represented by the Tan δ peak position corresponds to the T_g of the amorphous phases. It is interesting to note that the glass transition area of PB phases is more easily determined by DMA compared to DSC measurements. The T_g of HTPB can be viewed at −70°C for copolymers based on HTPB -R4 and at 0°C for copolymers based on HTPB -G3. However, DMA is less sensitive than DSC for the determination of the glass transition of amorphous PCL phases, since T_g of PCL blocks is not observed even for 80%w/w of PCL rate in the materials. The intensity of for neat PCL is small and no longer detectable for copolymers. This behavior could be attributed to the lower crystallinity of PCL developed in presence of high contents of HTPB as evidenced by DSC analysis. On the contrary, the intensity of Tan δ peak for HTPB phases increases in height with higher contents of HTPB in the copolymers.

3.2 Rheological Analysis

The measurements of rheological behaviors of polymeric materials at molten state are essential to gain fundamental understanding of the structure-property relation for these copolymers. The evolution of the rheological properties of these elastomeric block copolymers, depending on their chemical composition, are characterized by the measurement of the complex viscosity in relation to the temperature (Figs. 17–21). Complex viscosities values of the various

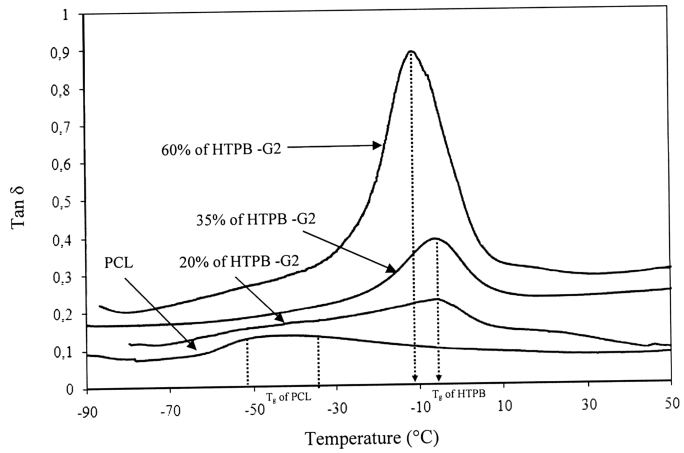

Fig. 13. Tan δ = f(T) for PB-PCL copolymers with different compositions in weight for PB and PCL synthesized with HTPB -G2.

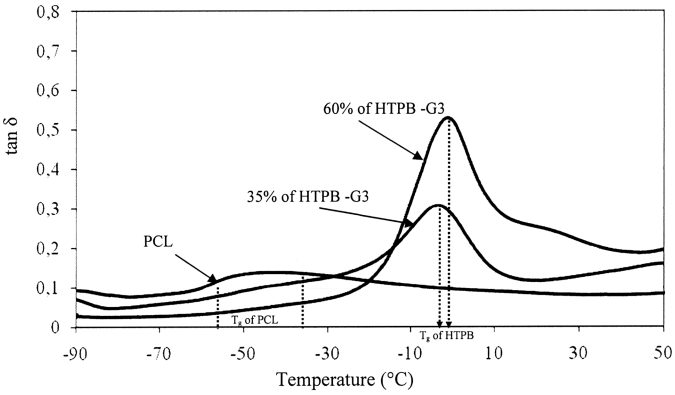

Fig. 15. Tan δ = f(T) for PB-PCL copolymers with different compositions in weight for PB and PCL synthesized with HTPB -G3.

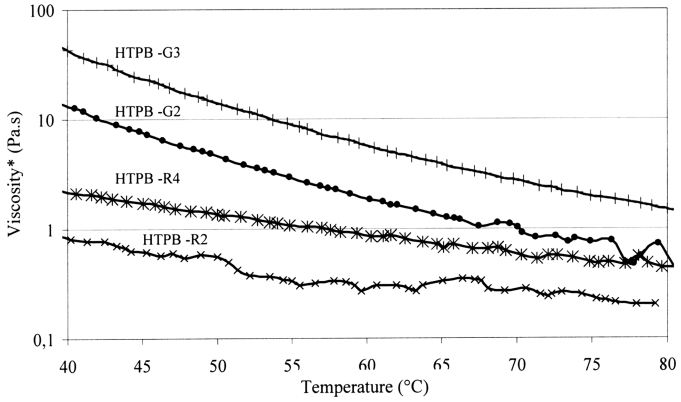

Fig. 16. Complex viscosity in relation to the temperature for the four used HTPB oligomers.

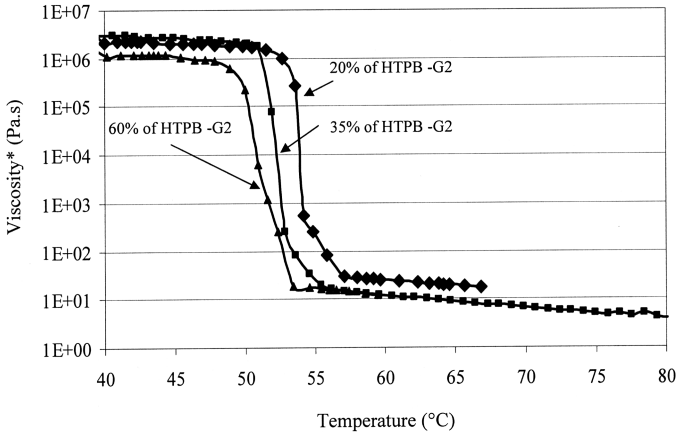

Fig. 19. Complex viscosity in relation to the temperature for HTPB -G2-PCL copolymers.

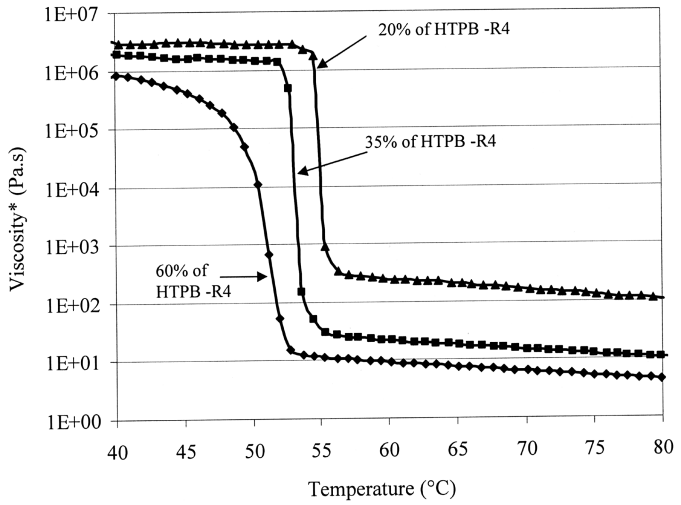

Fig. 17. Complex viscosity in relation to the temperature for HTPB -R4-PCL copolymers.

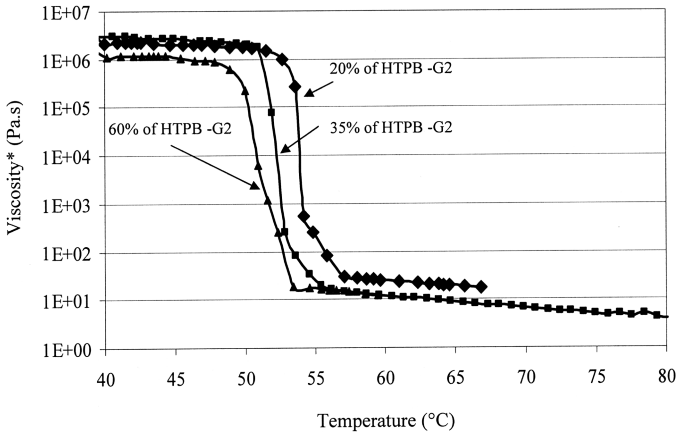

Fig. 20. Complex viscosity in relation to the temperature for HTPB -G3-PCL copolymers.

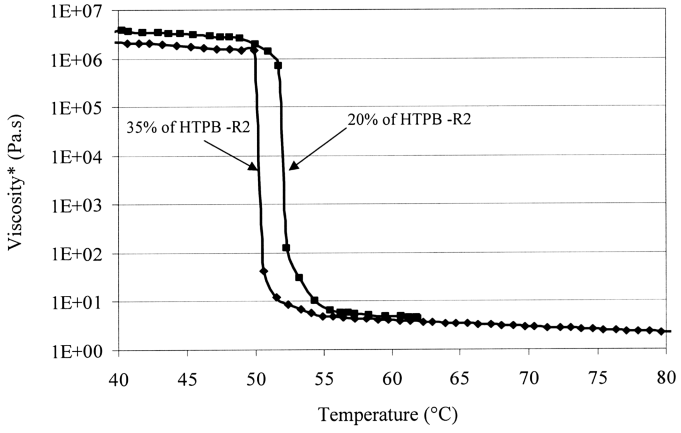

Fig. 18. Complex viscosity in relation to the temperature for HTPB -R2-PCL copolymers.

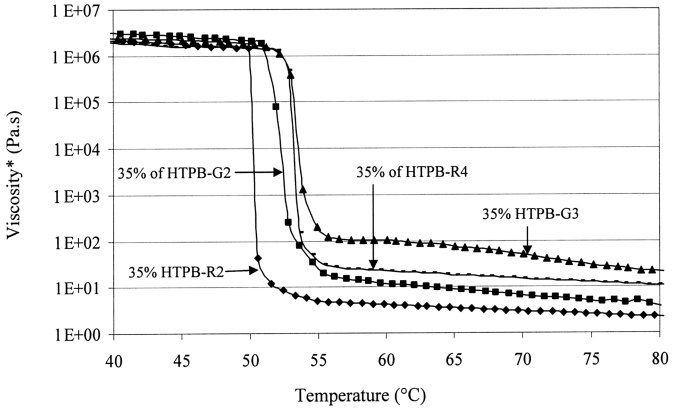

Fig. 21. Complex viscosity in relation to the temperature for PB-PCL copolymers with 35% w/w of various HTPB.

HTPB are typical for elastomeric oligomers (Fig. 16). In relation to microstructure variations, such as the 1–4 double bonds rate and the number molecular weight value, it is noteworthy that the complex viscosity of the G series is higher than that of the R series.

Rheological analyses of the various copolymers show an important decrease in the complex viscosity (decrease of at least three decades) of the materials when the PCL crystalline phase reaches the molten state, i.e., between 53°C and 58°C. For example, for the HTPB -R4 series (Fig. 17), the vitreous plateau is weakly affected by the PCL content. However, in the area of the PCL melting, the evolution is the same as the evolution detected by DSC or DMA analyses. Finally, the complex viscosity value, at the molten state, strongly depends on the length of the PCL blocks which is the highest for the 20% of HTPB -R4 copolymer. The control of the viscosity at the molten state, by the PCL content, and thus by the chains length, is common to all kinds of copolymers.

Moreover, Figure 21 shows that at a constant rate of PCL (65%) and PB (35%) in the copolymers, the molten state is also governed by the nature of the HTPB. For example, despite identical molecular weights ($\overline{M_n}$ = 20000 g/mol), the complex viscosity of the HTPB -G3 copolymer is higher than the complex viscosity of the HTPB -G2 copolymer. This can be related to the differences between the HTPB -G2 and -G3 viscosities displayed in Figure 16. It is interesting to note that a lower viscosity at the molten state can allow a better rearrangement of the macromolecular chains and thus an increase in the crystallinity rate of the materials as shown in Tables 5 and 6.

3.3 X-ray Diffraction

Figure 22 presents the diffractograms for three various copolymers based on HTPB -R4 containing 40% w/w, 65% w/w or 80% w/w of PCL as well as the diffractogram of neat PCL. The two diffraction rays characteristics of the PCL crystalline phases (31,32) for $2\theta = 22°$ and 24° are observed on the diffractograms of the three copolymers. Moreover, their intensities increase with the crystallinity rate of the copolymer. The orthorhombic (33,34) crystalline nature of the PCL phase is not modified when the content of PCL in the copolymer is modified. Finally, the large halo detected between 14° and 26° corresponds to the amorphous PB phases.

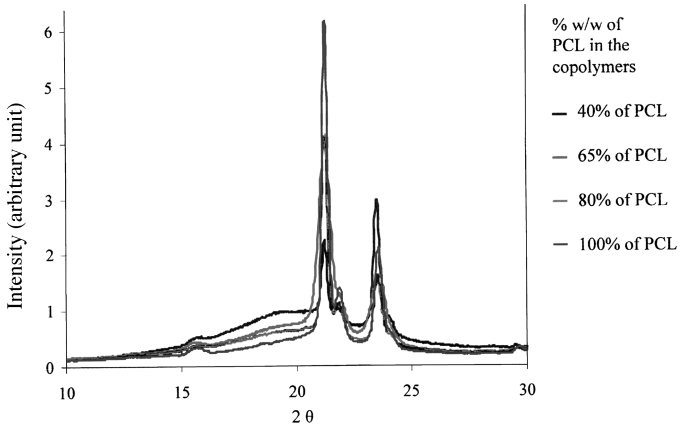

Fig. 22. Diffractograms of copolymers based on HTPB R45HT® and 40%, 65% and 80% of PCL and PCL homopolymer.

4 Conclusions

A broad series of tri- and multiblock copolymers based on linear and branched oligomers of polybutadiene (PB) as central blocks and polycaprolactone (PCL) as block extremities are characterized by SEC, DSC, DMA, Dynamical Rheology and DRX. DSC analyses reveal phase separation between the two amorphous PB and PCL phases. The general evolution of the thermal properties is similar for the copolymers based on the four kinds of HTPB. By thermal analysis, the glass transition temperature of PCL is only detected for materials containing at least 80% w/w of PCL. This is attributed to the small length of the polyester blocks for PCL/PB ratios under 80%w/w. The increase in fusion heat with increasing PCL content in the copolymers is correlated to the greater ability of PCL chains to rearrange when HTPB amount decreases in the material. Regarding the evolution of the melting temperature of the various copolymers, the characterization by DMA and dynamical rheology confirms the behavior observed by DSC. However, DMA appears to be less sensitive than DSC for the detection of the glass transition temperature of the polyester block. Mechanical and rheological properties (i.e., storage modulus and complex viscosities) reveal that the behavior of the copolymers depends on both the rate of PCL chains and the nature of the elastomeric block. These elastomers establish a large range of materials with modulated mechanical and thermal properties in relation to their chemical structure. They could be used for applications requiring a low processing temperature, as for example, in hot melt formulation.

References

1. Legge, N.R., Holden, G. and Schroeder, H.E. In Thermoplastic Elastomers. A Comprehensive Review, E. Editor, Hanser and Oxford University Press: Munich/New York, 1987.
2. Derouet, D., Nguyen Tran Minh, G. and Brosse, J.C. (2007) *J. Appl. Polym. Sci.,* 1065, 2843–2858.
3. Coltelli, M.B., Della Maggiore, I., Savi, S., Aglietto, M. and Ciardelli, F. (2005) *Polym. Degrad. Stabil.*, 90, 211–23.
4. Tanrattanakul, V., Perkins, W.G., Massey, F.L., Moet, A., Hiltner, A. and Baer, E. (1997) *J. Mater. Sci.*, 32, 4749–58.
5. Gupta, A.K. and Purwar, S.N. (1984) *J. Appl. Polym. Sci.,* 29, 3513–3531.
6. Gupta, A.K. and Purwar, S.N. (1984) *J. Appl. Polym. Sci.*, 29, 1595–1609.

7. Stricker, F., Thomann, Y. and Mülhaupt, R. (1998) *J. Appl. Polym. Sci*., 68, 1891–1901.
8. Wilhelm, H.M. and Felisberti, M.I. (2002) J. Appl. Polym. Sci., 86, 359–365.
9. Wang, Y., Yang, R., Han, Y., Wang, J., Liu, M., Quan, G. and Liu, A. Patent 2009, CN 101423749 A 20090506.
10. Lim, D.H., Park, Y.J. and Kim, H.J. Nippon Setchaku Gakkai Nenji Taikai 2005; 43rd. p. 65–66.
11. Adams, J., LaMonte, G., William, W. and Register, R.A. (1994) *Macromolecules*, 2721, 6026–32.
12. Wilkinson, A.N., Clemens, M.L. and Harding, V.M. (2004) *Polymer*, 45, 5239–5249.
13. Nishitani, Y., Yamada, Y., Ishii, C., Sekiguchi, I. and Kitano, T. (2010) *Polym. Eng. Sci.*, 501, 100–112.
14. Picchioni, F., Aglietto, M., Passaglia, E. and Ciardelli, F. (2002) *Polymer*, 4311, 3323–3329.
15. Ryynanen, T., Nykanen, A. and Seppala, J.V. (2008) *Express Polym. Let*., 23, 184–193.
16. Gelles, R., Dubois, D.A. and St. Clair, D.J. U.S. Pat. Appl. Publ. 2009; US 2009093584 A1 20090409.
17. Scheiber, P., Eur. Pat. Appl. 2009; EP 2112721 A1 20091028.
18. Fakhraian, H., Anbaz, K., Babaei Panbeh Riseh, M. and Ghafouri, M. (2009) *Int. J. of Adhesion and Adhesives*, 292, 111–113.
19. Balsamo, V., Gildenfeldt, F. and Stadler, R. (1996) *Macromol. Chem. Phys*., 197, 1159–1169.
20. Rozenberg, B.A., Estrin, Y.I. and Estrina, G.A. (2000) *Macromol. Symp*., 1531, 197–208.
21. Lemoine, M., Brachais, C.H., Boni, G. and Couvercelle, J.P. (2009) e-Polymers, no. 032.
22. Meng, F., Zheng, S., Zhang, W., Li, H. and Liang, G. (2006) *Macromolecules,* 39, 711–719.
23. Nojima, S. and Akaba, M. (2006) *Polym. J.,* 38, 559–566.
24. Nojima, S., Nakano, H., Takahashi, Y. and Shida, T. (1994) *Polymer,* 35, 3479–3485.
25. Kim, G., Jackson, C.L., Balsamo, V., Libera, M., Stadler, R. and Han, C.C. Abstracts of papers, 57th Annual Technical Conference of the Society of Plastics Engineers, 1999; 2, 1734–1738.
26. Balsamo, V., Von Gyldenfeldt, F. and Stadler, R. (1999) *Macromolecules*, 32, 1226–1232.
27. Jackson, C.L., Chanzy, H.D., Han, C., Balsamo, V., Von Gyldenfeldt, R. and Stadler, R. Abstracts of papers, 214th ACS National Meeting in Las Vegas, NV, 1997; p. MACR–054.
28. Yam, W.Y., Ismail, J., Kammer, H.W., Schmidt, H. and Kummerlowe, C. (1999) *Polymer*, 40, 5545–5552.
29. Takizawa, K., Tang, C. and Hawker, C.J. (2008) *J. Am. Chem. Soc.*, 130, 1718–1726.
30. Poussard, L. PhD thesis, University of Rouen, 2005.
31. Nishio, Y. and Manley, R.StJ. (1990) *Polym. Eng. Sci.,* 302., 71–82.
32. Huarng, J.C., Min, K. and White, J.L. (1988) *Polym. Eng. Sci*., 28, 1590–1599.
33. Bittiger, H., Marchessault, R.H. and Niegisch, W.D. (1970) *Acta Cryst*., 2612, 1923–1927.
34. Chatani, Y., Okita, Y., Tadokoro, H. and Yamashita, Y. (1970) *Polymer*, 15, 555–562.